PHYSICS AND CHEMISTRY OF SOLID STATE
V. 23, No. 2 (2022) pp. 235-241
Section: Physics

DOI: 10.15330/pcss.23.2.235-241

Vasyl Stefanyk Precarpathian National University

ФІЗИКА І ХІМІЯ ТВЕРДОГО ТІЛА
Т. 23, № 2 (2022) С. 235-241
Фізико-математичні науки

UDC 537.311.322 ISSN 1729-4428

V.A. Romaka[1], Yu. Stadnyk[2], L. Romaka[2], A. Horyn[2], V. Pashkevich[1], H. Nychyporuk[2], P. Garanyuk[1]

Investigation of Thermoelectric Material Based on $Lu_{1-x}Zr_xNiSb$ Solid Solution. I. Experimental Results

[1]*Lviv Polytechnic National University, Lviv, Ukraine, volodymyr.romaka@gmail.com;*
[2]*Ivan Franko L'viv National University, L'viv, Ukraine, lyubov.romaka@gmail.com*

The effect of doping of half-Heusler phase *p*-LuNiSb (MgAgAs structure type) by Zr atoms on the structural, kinetic, energetic and magnetic characteristics of the semiconductor solid solution $Lu_{1-x}Zr_xNiSb$ was studied in the ranges: T = 80 - 400 K, x = 0 - 0.10. From experimental studies it has been established that doping of *p*-LuNiSb compound with Zr atoms simultaneously generates both structural defects of acceptor and donor nature, the concentration of which increases with increasing content of Zr atoms. It was shown that the investigated semiconductor solid solution $Lu_{1-x}Zr_xNiSb$ is a promising thermoelectric material.

Keywords: semiconductor, electrical conductivity, thermopower coefficient, Fermi level.

Received 27 September 2021; Accepted 18 April 2022.

Introduction

Solid solutions based on half-Heusler phases RNiSb (R- rare earth metals of Yttrium subgroup) [1] which crystallize in the MgAgAs structure type (space group $F\bar{4}3m$) [2] are insufficiently studied, but a promising class of semiconductor thermoelectric materials with high efficiency of conversion of thermal energy into electricity. The structural, electrokinetic, and magnetic characteristics of RNiSb compounds ((R = Gd, Tb, Dy, Yb, Lu) were studied in Refs. [3, 4]. The authors found that the crystal structure of the compound $YbNi_{0.9}Sb$ is defective, and the studied compounds are semiconductors of the hole-type conductivity. Defects in the crystal structure were also found for half-Heusler compounds $ScNi_{0.87}Sb$ and $ScPd_{0.96}Sb$, which are characterized by the presence of vacancies in the positions of the transition metal [5]. Thus, in the crystal, there is a mechanism for generating structural defects of acceptor nature. However, the authors did not propose the structure model and mechanism of defect generation that would adequately explain the results of experimental studies, in particular, for the LuNiSb compound.

This problem was solved in Refs. [6, 7]. Taking into account the results of measurements of temperature dependences of electrical resistivity ρ, thermopower coefficient α, and magnetic susceptibility χ, the method of iterative modeling of structural, energetic, thermodynamic, and kinetic characteristics of materials was used to establish a model of crystal and electronic structures of LuNiSb compound [1]. Calculations of the density distribution of electronic states DOS were performed for different variants of the arrangement of atoms in the nodes of the unit cell and the occupancy of crystallographic positions by their own and/or foreign atoms. We looked for the compensation degree of *p*-LuNiSb, which will provide an experimentally established position of the Fermi level ε_F relative to the top of the valence band. Simulation of the electronic structure of *p*-LuNiSb showed that the band gap ε_g appears only in the presence of vacancies (Va) (~ 6 %) in the crystallographic position 4*c* of Ni atoms. In this case, structural defects of acceptor nature are generated in the crystal, and acceptor levels (band) $\varepsilon_A{}^1$ appear in the band gap ε_g. This is the mechanism of "a priori doping" of the *p*-LuNiSb semiconductor by acceptor impurities [1].

On the other hand, one of the ways to obtain thermoelectric materials with high values of the figure of

merit Z is to generate in the crystal structural defects of donor and/or acceptor nature, which simultaneously leads to changes in the values of thermopower coefficients $\alpha(T,x)$ and thermal conductivity $\kappa(T,x)$, as well as the electrical conductivity $\sigma(T,x)$ [8].

That is why, to obtain a new effective thermoelectric material, we began the study of a semiconductor solid solution $Lu_{1-x}Zr_xNiSb$ synthesized by doping LuNiSb compound with Zr atoms by substitution of Lu atoms in the 4*a* crystallographic position. In this case, structural defects of donor nature should be generated in the semiconductor, because Zr ($4d^25s^2$) contains more *d*-electrons than the Lu atom ($5d^16s^2$). Above we focused on the results of the crystal and electronic structure studies of *p*-LuNiSb [6, 7] because knowledge of the atom distribution in the LuNiSb compound will allow us to understand the mechanism of including Zr atoms into the structure to obtain the solid solution $Lu_{1-x}Zr_xNiSb$. The first results of the study of structural, kinetic, energetic, and magnetic characteristics of the semiconductor solid solution $Lu_{1-x}Zr_xNiSb$, x = 0 - 0.10, presented below, will allow us to identify the mechanisms of electrical conductivity and further refine its crystal and electronic structure.

I. Methods and materials

Alloys of $Lu_{1-x}Zr_xNiSb$ solid solution, x = 0.01 - 0.10, were synthesized by an arc melting of components weighed with an accuracy of ± 0.001 g in an electric arc furnace with a tungsten electrode (cathode) in an atmosphere of purified argon at a pressure of 0.1 kPa on a water-cooled copper bottom (anode). Spongy titanium was used as a getter. The alloys were re-melted twice to achieve homogeneity. Control of charge losses during melting was performed by repeated weighing. Heat treatment of alloys consisted of homogenizing annealing at 1073 K. Annealing of the samples was performed for 720 h in evacuated up to 1.0 Pa quartz ampoules in muffle electric furnaces with temperature control with an accuracy of ± 10 K. Powder diffraction data were obtained on a powder diffractometer DRON-4.0 (FeKα radiation), and the structural characteristics of $Lu_{1-x}Zr_xNiSb$ were calculated using the Fullprof Suite program package [9]. The chemical and phase compositions of the samples were examined by metallographic analysis (scanning electron microscope Tescan Vega 3 LMU).

The study of the temperature dependences of the resistivity $\rho(T,x)$ and the thermopower coefficient $\alpha(T,x)$ of $Lu_{1-x}Zr_xNiSb$ was performed in the temperature range from 80 K to 400 K on the samples in the form of rectangular parallelepipeds with dimension ~1.0×1.0×5 mm^3. Measurement of electrical resistivity was carried out using the two-probe method, and the thermopower coefficient was measured by the potentiometric method with pure copper as reference material. To reduce "parasitic" effects caused by the influence of thermopower in place of contact and the effects caused by the possible impact of a *p-n* junction, the measurement of the voltage drop on the sample performed at different directions of electric current [10]. Measurements of the values of the specific magnetic susceptibility χ of $Lu_{1-x}Zr_xNiSb$ samples were performed by the relative Faraday method at 293 K using a thermogravimetric instrument with an electronic microbalance in magnetic fields up to 10 kOe.

II. Study of structural characteristics of $Lu_{1-x}Zr_xNiSb$

Microprobe analysis of the atom concentration on the surface of $Lu_{1-x}Zr_xNiSb$ samples, x = 0 - 0.10, established their correspondence to the initial compositions of the charge, and X-ray phase analysis showed no traces of impurity phases on the powder patterns, except for the main phase (Fig. 1a), which is indexed in the MgAgAs structure type [2].

Based on the fact that the atomic radius of Lu (r_{Lu} = 0.173 nm) is larger than Zr (r_{Zr} = 0.160 nm), it was logical to expect a decrease in the lattice parameter values $a(x)$ of $Lu_{1-x}Zr_xNiSb$ samples by substituting of Lu atoms at 4*a* position for Zr atoms. In this case, as mentioned above, structural defects of donor nature should be generated in the crystal, and donor levels (band) ε_D^1 will appear in the band gap.

However, as seen from Fig. 1b, in the concentration range x = 0–0.02 the values $a(x)$ of $Lu_{1-x}Zr_xNiSb$ increase

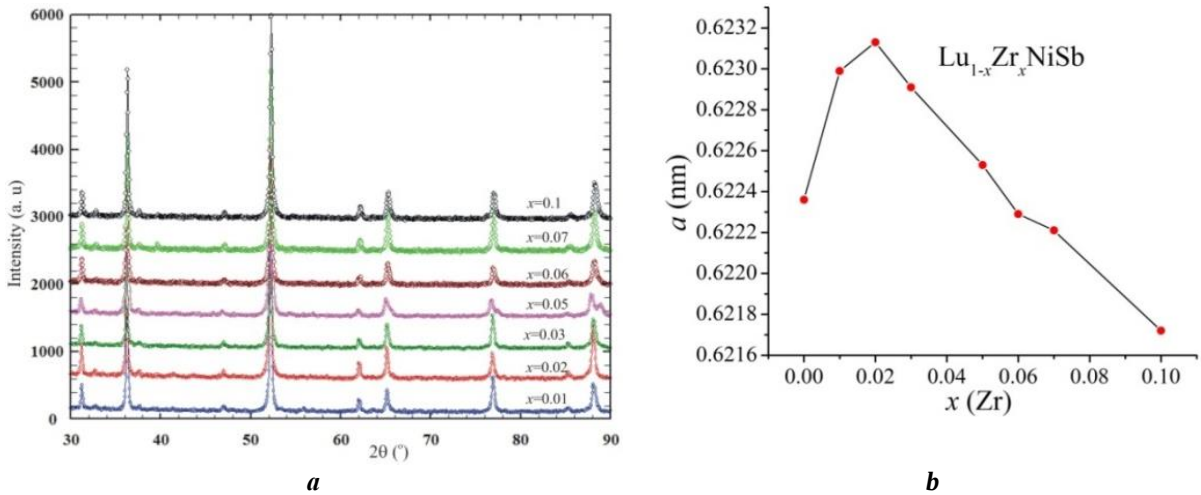

a ***b***

Fig. 1. Powder patterns (**a**) and variation of the lattice parameter $a(x)$ (**b**) of $Lu_{1-x}Zr_xNiSb$ samples.

rapidly, pass through the maximum, and at $x > 0.02$ decrease rapidly too. It should be noted that in a related semiconductor solid solution $Er_{1-x}Zr_xNiSb$ we observed a similar behavior of the lattice parameter $a(x)$, where the values $a(x)$ increase in the range $x = 0 - 0.02$, and they decrease at $x > 0.05$ [11].

The nonmonotonic change of the lattice parameter values $a(x)$ of $Lu_{1-x}Zr_xNiSb$ (Fig. 1*b*) and the presence of an extremum on $a(x)$ dependence suggests that the impurity Zr atoms introduced into the matrix of the half-Heusler phase LuNiSb, can simultaneously in different ratios partially occupy different crystallographic positions and generate the appearance of vacancies or atoms in the tetrahedral voids of the structure, which make up ~ 24 % of the volume of the unit cell [2].

Taking into account that the atomic radius of the Ni atom ($r_{Ni} = 0.124$ nm) is the smallest among the chemical elements of the solid solution $Lu_{1-x}Zr_xNiSb$ ($r_{Sb} = 0.159$ nm), the increase of the lattice parameter values $a(x)$ can be caused by the partial occupation of impurity Zr atoms in the crystallographic 4*c* position of Ni atoms. In addition, it is likely that Ni will return to this position, which will lead to the elimination of vacancies. And if the substitution of Lu atoms by Zr atoms in position 4*a* generates structural defects of donor nature in the crystal, then the substitution of Ni atoms ($3d^8 4s^2$) by Zr atoms ($4d^2 5s^2$) is accompanied by the generation of structural defects of acceptor nature, because Zr atom contains fewer *d*-electrons. At the same time, another acceptor levels (band) $\varepsilon_A{}^2$ should appear in the band gap of $Lu_{1-x}Zr_xNiSb$. In this case, the semiconductor $Lu_{1-x}Zr_xNiSb$, $x = 0 - 0.02$, will simultaneously contain donors and acceptors, and their ratio will determine the sign of the thermopower coefficient $\alpha(x,T)$ and the type of main current carriers.

On the other hand, if we remind that the structural defects in the form of vacancies in the crystallographic position 4*c* caused the appearance of acceptor levels (bands) $\varepsilon_A{}^1$ in the band gap of the *p*-LuNiSb semiconductor [7, 8], then the occupation of vacancies by Ni or Zr atoms in position 4*c*, as well as the replacement of Ni atoms by Zr, will increase the lattice parameter values $a(x)$ of $Lu_{1-x}Zr_xNiSb$. In the case of occupation of vacancies in position 4*c* by Zr or Ni atoms, the generation of structural defects of donor nature takes place, and two impurity donor levels will appear in the band gap. At the same time, the structural defect of acceptor nature (vacancy) and the corresponding acceptor level (band) $\varepsilon_A{}^1$ disappear.

We are aware that the above considerations regarding the possible transformations of the structural and energy characteristics of the solid solution $Lu_{1-x}Zr_xNiSb$ based only on the behavior of the lattice parameter $a(x)$ are of a qualitative nature. The presented below results of the study of electrokinetic, energetic and magnetic characteristics of $Lu_{1-x}Zr_xNiSb$ samples, $x = 0 - 0.10$, will serve as reference points in the future, which we will use to model the electronic structure of the solid solution, in particular, the transformation of energy bands and Fermi level ε_F, and also simulating of structural, kinetic and energetic characteristics as close as possible to the real state of matter. However, this is the task of the next work.

III. Study of electrokinetic, energetic and magnetic characteristics of $Lu_{1-x}Zr_xNiSb$

The temperature and concentration dependencies of electrical resistivity ρ and thermopower coefficient α *of* $Lu_{1-x}Zr_xNiSb$ samples, $x = 0 - 0.10$, are shown in Figs. 2-4.

As can be seen from Fig. 2, for the initial compound *p*-LuNiSb, the $\ln(\rho(1/T))$ dependence is characteristic of semiconductors [12] and is approximated by the known relation (1):

$$\rho^{-1}(T) = \rho^{-1} exp\left(\frac{\varepsilon_1^\rho}{k_B T}\right) + \rho_3^{-1} exp\left(\frac{\varepsilon_3^\rho}{k_B T}\right), \qquad (1)$$

where the first high-temperature term describes the activation of current carriers ε_1^ρ from the Fermi level ε_F to the level of continuous energy bands, and the second low-temperature one, is the hopping conductivity within impurity donor states ε_3^ρ with energies close to the Fermi level ε_F. Performed calculations showed that in the studied sample *p*-LuNiSb the Fermi level ε_F is located at the distance $\varepsilon_1^\rho = 10.2$ meV from the top of the valence band ε_V.

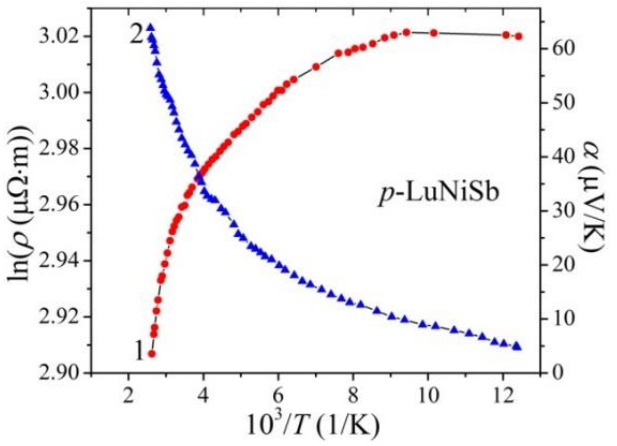

Fig. 2. Temperature dependencies of electrical resistivity $\ln(\rho(1/T))$ (1) and thermopower coefficient $\alpha(1/T)$ (2) for p-LuNiSb.

In turn, the temperature dependences of the thermopower coefficient $\alpha(1/T)$ of *p*-LuNiSb (Fig. 2) are described by the known expression (2) [13]:

$$\alpha = \frac{k_B}{e}\left(\frac{\varepsilon_i^\alpha}{k_B T} - \gamma + 1\right), \qquad (2)$$

where γ is a parameter that depends on the nature of the scattering mechanism. From the high- and low-temperature activation parts of the $\alpha(1/T)$ dependence, the values of activation energies $\varepsilon_1^\alpha = 35.3$ meV and $\varepsilon_3^\alpha = 1.9$ meV were calculated, respectively. As shown in [1], they are proportional to the amplitude of large-scale fluctuations of continuous energy bands and small-scale fluctuations of heavily doped and highly compensated semiconductor (HDHCS) [12].

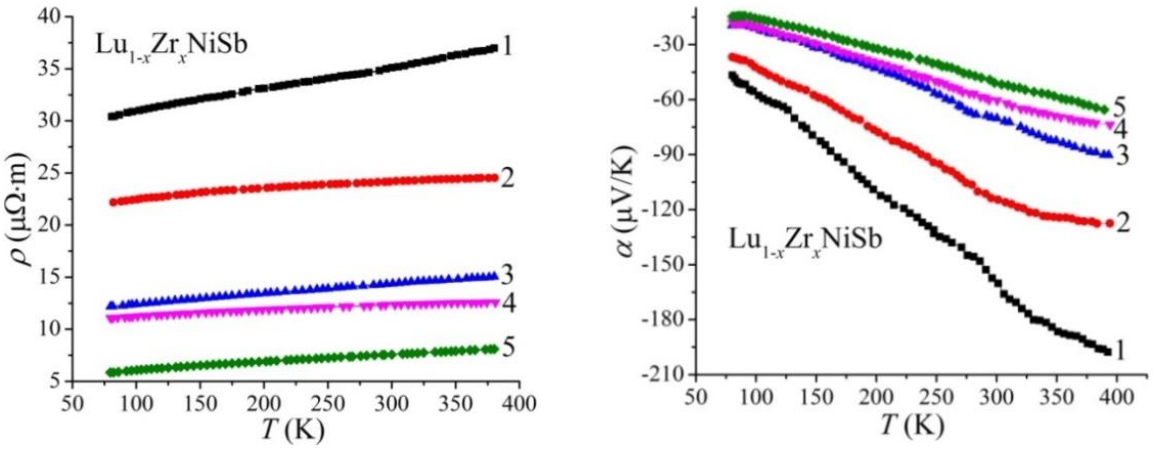

a *b*

Fig. 3. Temperature dependencies of electrical resistivity $\rho(T,x)$ (**a**) and thermopower coefficient $\alpha(T,x)$ (**b**) of $Lu_{1-x}Zr_xNiSb$: 1 – x = 0.01; 2 – x = 0.02; 3 – x = 0.05; 4 – x = 0.07; 5 – x = 0.1.

The presence of a high-temperature activation part on the temperature dependence of the resistivity $\ln(\rho(1/T))$ of *p*-LuNiSb indicates the location of the Fermi level ε_F in the band gap ε_g of the semiconductor, and the positive values of the thermopower coefficient $\alpha(T,x)$ at these temperatures specify its position near the valence band ε_V. Thus, holes are the main carriers of electric current. The obtained values of activation energies ε_1^{ρ} and ε_1^{α} for *p*-LuNiSb are consistent with the results of previous studies [1].

In this context, it is interesting to note the "portion" of Ni atoms that are absent in the crystallographic position 4*c*, which creates vacancies in this position and acceptor levels (band) $\varepsilon_A{}^1$ in the band gap ε_g of the *p*-LuNiSb semiconductor [6, 7]. Since during the synthesis of LuNiSb samples, the charge was prepared according to the equiatomic composition of the compound, and microprobe analysis of the concentration of atoms on the surface of the samples established their correspondence to the initial compositions of the charge, then where did ~ 6 % of Ni atoms go?

We can assume that a significant part of them is placed in the tetrahedral voids of the structure, which make up ~ 24 % of the volume of the unit cell [2], generating structural defects of donor nature. Exactly the concentration ratio of ionized acceptors generated by vacancies in the 4*c* site and donors (Ni atoms are in tetrahedral voids) determines the position of the Fermi level ε_F in the band gap ε_g of the *p*-LuNiSb semiconductor. After all, the absence of compensating donors in *p*-LuNiSb at a giant concentration of acceptors (~ 6 %) would lead to the location of the Fermi level ε_F deep into the valence band ε_V and the complete metallization of electrical conductivity. However, according to experimental data, the Fermi level in *p*-LuNiSb lies in the band gap ε_g near the top of the valence band ε_V, which can be caused only by the presence in the crystal compensating structural defects of donor nature. These are Ni atoms in tetrahedral voids, as we consider.

Doping of *p*-LuNiSb with the lowest concentration of impurity Zr atoms in the experiment (x = 0.01) radically changes both the nature of the behavior of temperature dependences of resistivity ρ and thermopower coefficient α, and the type of main carriers of electric current (Fig. 3). The metallic (non-activating) behavior of temperature dependences of the resistivity $\rho(T,x)$ of $Lu_{1-x}Zr_xNiSb$ (Fig. 3a) indicates that the Fermi level ε_F has left the band gap ε_g and is located in the continuous energy band. The fact that this is the conduction band of the semiconductor ε_C can be stated on the basis on negative values of the thermopower coefficient $\alpha(T,x)$ (Fig. 3b) at all concentrations and temperatures. It is clear that the increase of the $\rho(T,x)$ values of $Lu_{1-x}Zr_xNiSb$ with increasing temperature is due to the scattering mechanisms of current carriers in the semiconductor.

The obtained result, especially the complete metallization of the electrical conductivity of $Lu_{1-x}Zr_xNiSb$ even at the lowest impurity concentration, was completely unexpected. According to our estimates, if in the crystallographic position 4*a* the Lu atoms were replaced by Zr atoms and only donors were generated in the semiconductor, then at the concentration $x \approx 0.02$, the Fermi level ε_F should be near the middle of the band gap ε_g. In this case, high-temperature activation parts would be present at the temperature dependences of the resistivity, indicating the activation of current carriers from the Fermi level ε_F to the continuous energy bands. Thus, at $x < 0.02$ the sign of the thermopower coefficient $\alpha(T,x)$ would be positive, because the Fermi level ε_F was closer to the top of the valence band and holes are the main current carriers, and at $x > 0.02$ - negative. And only at concentrations $x > 0.04$ the Fermi level ε_F should cross the bottom of the conduction band ε_C, which would lead to the disappearance of activation parts on the temperature dependences of the resistivity $\ln(\rho(1/T))$ of $Lu_{1-x}Zr_xNiSb$ and metallization of conductivity.

As a result, the character of change of the resistivity values $\rho(x,T)$ for $Lu_{1-x}Zr_xNiSb$ at all temperatures was also unexpected (Fig. 4a). If two types of electric current carriers are present in a semiconductor simultaneously, then the maximum on the dependence $\rho(x,T)$ indicates that the concentrations of the available ionized acceptors and donors are balanced. In the case of $Lu_{1-x}Zr_xNiSb$, we expected such a maximum at concentration $x \approx 0.02$. Available in Fig. 4a maximum $\rho(x,T)$ for $Lu_{1-x}Zr_xNiSb$ $x \approx 0.01$ has nothing to do with the stated opinion. After all, for x = 0 we have a semiconductor of hole-type conductivity when the Fermi level ε_F lies at the distance of

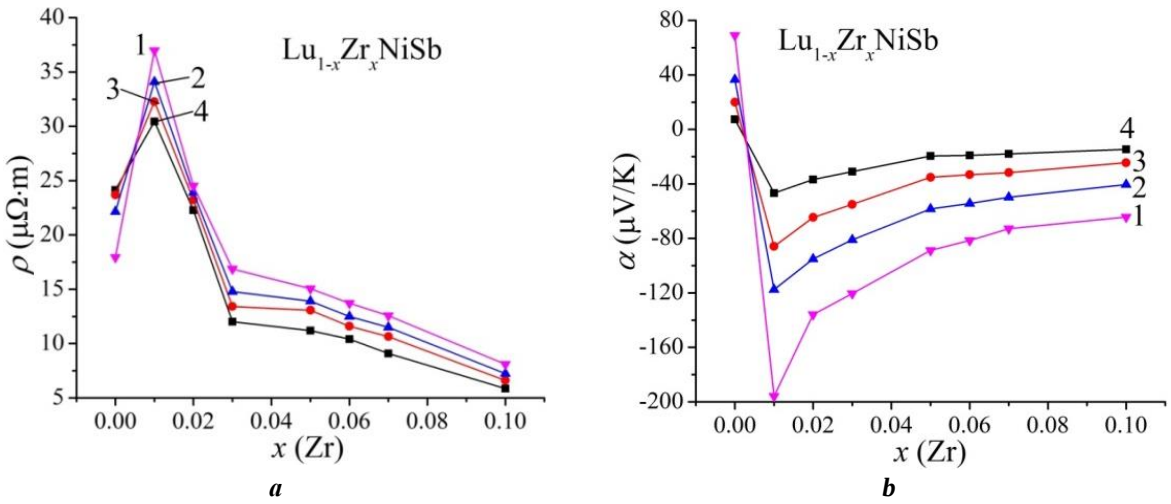

a ***b***

Fig. 4. Variations of the electrical resistivity values $\rho(T,x)$ (**a**) and thermopower coefficient $\alpha(T,x)$ (**b**) for $Lu_{1-x}Zr_xNiSb$ at different temperatures: 1 – T = 380 K; 2 – T = 250 K; 3 – T = 160 K; 4 – T = 80 K.

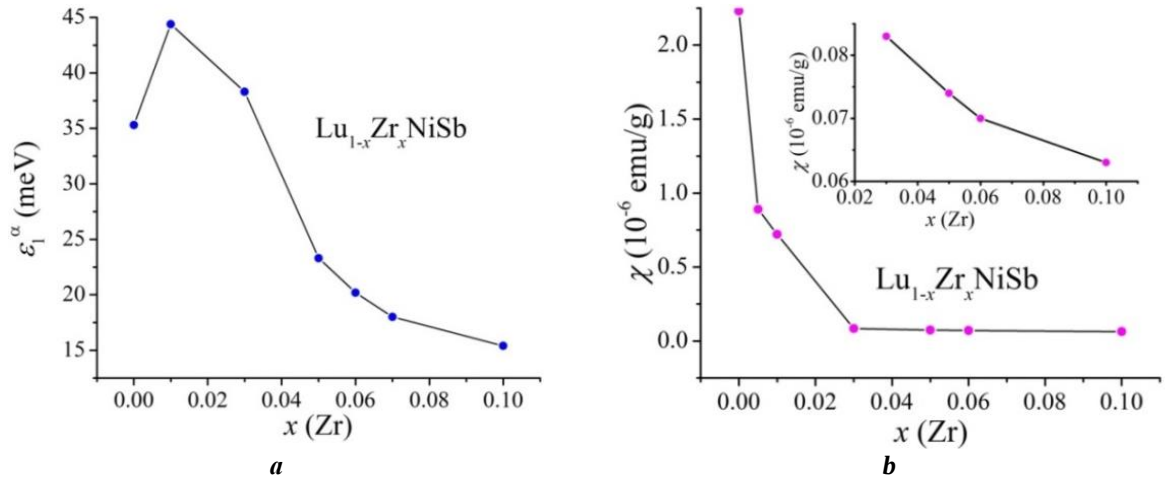

a ***b***

Fig. 5. Variations of the activation energy values $\varepsilon_1^{\alpha}(x)$(**a**) and magnetic susceptibility values $\chi(x)$(**b**) of $Lu_{1-x}Zr_xNiSb$ at T = 293 K.

10.2 meV from the edge of the valence band ε_V, and at the concentration x = 0.01 it is located deep in the conduction band ε_C and electrons are the main current carriers. The same applies to the character of change of thermopower coefficient values $\alpha(x,T)$ for $Lu_{1-x}Zr_xNiSb$, in particular, the available minimum at $x \approx 0.01$ (Fig. 4b). It is correct to take into account only the decrease of $\rho(x,T)$ values and the increase of $\alpha(x,T)$ values for $Lu_{1-x}Zr_xNiSb$ in the concentration range $0.01 \le x \le 0.10$ at all temperatures (Fig. 4), which indicates an increase of electron concentration and density of states at the Fermi level $g(\varepsilon_F)$. This is clear, because Zr atoms, replacing Lu, generate structural defects of donor nature, which supply electrons to the semiconductor.

The results of activation energies $\varepsilon_1^{\alpha}(x)$ calculation (Fig. 5a) from low-temperature activation parts of the $\alpha(1/T)$ dependences of $Lu_{1-x}Zr_xNiSb$ were very interesting and informative. The activation energy values are proportional to the amplitude of large-scale fluctuations of the continuous energy bands of HDHCS, caused by the fluctuation nature of the location in the crystal of charged centers, in particular, ionized acceptors and donors [12].

The higher compensation degree of semiconductors (ratio of ionized acceptors and donors) causes greater distortions of the continuous energy bands and the value of the modulation amplitude of the continuous energy bands. It should be noted that the analysis of the behavior of the activation energy $\varepsilon_1^{\alpha}(x)$ of $Lu_{1-x}Zr_xNiSb$ is correct only in the concentration range $0.01 \le x \le 0.10$, when one type of the main carriers determines the conductivity of the semiconductor. After all, at $x = 0$ we have a semiconductor of hole type conductivity, and at $x \ge 0.01$ – electron type.

As seen from Fig. 5a, at concentrations $0.01 \le x \le 0.10$, the activation energy values $\varepsilon_1^{\alpha}(x)$ of $Lu_{1-x}Zr_xNiSb$ decrease rapidly, indicating the predominance of the concentration of one type of electric current carriers over another. Since the main current carriers of $Lu_{1-x}Zr_xNiSb$ at $x \ge 0.01$ are electrons and their concentration is much higher than that of holes, the ratio of donors to holes increases with increasing impurity concentration (compensation degree decreases).

In the classical case of doping, for example, a *p*-type semiconductor by a donor impurity, first it leads to the capture of free electrons by acceptors (ionization of acceptors) to concentrations when the number of acceptors corresponds to the number of ionized donors. At higher concentrations, when all acceptors are ionized, the electrons supplied by donors become collective (free) and participate in electrical conductivity. That is, initially the

electrons are captured by the acceptors available in the semiconductor [10].

The question of the reason for such nonclassical behavior of the kinetic characteristics of $Lu_{1-x}Zr_xNiSb$ seems logical. That is, what structural changes in the $Lu_{1-x}Zr_xNiSb$ solid solution could have caused such a significant effect on the electronic system of the semiconductor, which is reflected in the described above electrokinetic characteristics?

As noted above, there are simultaneously ~ 6 % of vacancies in the position of 4*c* of Ni atoms in the structure of *p*-LuNiSb, which generates structural defects of acceptor nature, and the corresponding acceptor level (band) ε_A^1 appears in the band gap ε_g. In addition, structural studies of $Lu_{1-x}Zr_xNiSb$ showed that the increase of the lattice parameter values $a(x)$ in the concentration range x = 0 - 0.02 (Fig. 1b) is caused by the occupation of impurity Zr atoms of vacancies in the structure. Herewith the structural defects of donor nature are generated, and another impurity donor level (band) ε_D^2 will appear in the band gap. At the same time, the structural defect of acceptor nature (vacancy) in position 4*c* and the corresponding acceptor level (band) ε_A^1 disappear.

Thus, the simultaneous disappearance of acceptors (not compensation by electrons, but exactly disappearance) and the inclusion of three mechanisms for generating donors:

- occupation of the crystallographic position 4*c* (vacancies) by Zr atoms;
- substitution of Lu atoms by Zr atoms in the crystallographic position 4*a*;
- occupation of tetrahedral voids of the structure by Zr atoms is the reason for the appearance in the $Lu_{1-x}Zr_xNiSb$ semiconductor of a giant concentration of donors, which caused the location of the Fermi level ε_F in the conduction band ε_C, an increase of the density of states at the Fermi level $g(\varepsilon_F)$ and metallization of electrical conductivity.

Experimental studies of the magnetic susceptibility $\chi(x)$ have shown that samples of both LuNiSb compound and $Lu_{1-x}Zr_xNiSb$ solid solution at all concentrations are Pauli paramagnets (Fig. 5b). In this case, the similar behavior of the dependences of the resistivity $\rho(x,T)$ (Fig. 4a), the thermopower coefficient $\alpha(x,T)$ (Fig. 4b) and the magnetic susceptibility $\chi(x)$ (Fig. 5b) is associated with a change of the density of states at the Fermi level $g(\varepsilon_F)$.

Therefore, the study of $Lu_{1-x}Zr_xNiSb$ semiconductive solid solution obtained by doping of LuNiSb compound with Zr atoms by substituting Lu atoms in the crystallographic position 4*a* showed the complex nature of the introduction of impurity atoms into the compound matrix when changes occur simultaneously in several crystallographic positions and internodes of the crystal. However, this issue requires additional research, in particular structural, and modeling of the electronic structure of the $Lu_{1-x}Zr_xNiSb$ semiconductive solid solution under different conditions of including impurity Zr atoms into the structure. The obtained experimental results will serve as reference points in the calculations, which will be the aim of the next work.

Conclusions

Consequently, based on the results of the study of structural, kinetic, energetic, and magnetic characteristics of $Lu_{1-x}Zr_xNiSb$ solid solution samples, x = 0 - 0.10, it was established that to ensure the stability of the structure and the principle of electroneutrality in the semiconductor both structural defects of acceptor and donor nature (effective charge of which is the opposite) are simultaneously generated. The concentration of acceptor and donor increases with the increasing content of Zr atoms. The investigated solid solution $Lu_{1-x}Zr_xNiSb$ is a promising thermoelectric material.

Acknowledgements

We would like to acknowledge financial support of the Ministry of Education and Science of Ukraine under Grant No. 0121U109766.

RomakaV. – Proffesor, PHD;
Stadnyk Yu. **–** Ph.D., Senior Scientist;
Romaka L. **–** Ph.D., Senior Scientist;
Horyn A. **–** Ph.D., Senior Scientist;
Pashkevych V. **–** docent;
Nychyporuk H. – Ph.D., Senior Scientist;
Garanyuk P. **–** docent.

[1] V.A. Romaka, Yu.V. Stadnyk, V.Ya. Krayovskyy, L.P. Romaka, O.P. Guk, V.V. Romaka, M.M. Mykyychuk, A.M. Horyn, The latest heat-sensitive materials and temperature transducers (Lviv Polytechnic Publishing House, Lviv, 2020); ISBN 978-966-941-478-6 [in Ukrainian].
[2] V.V. Romaka, L.P. Romaka, V.Ya. Krayovskyy, Yu.V. Stadnyk, Stannides of rare earths and transition metals (Lviv Polytechnic Publishing House, Lviv, 2015); ISBN 978-617-607-816-6 [in Ukrainian].
[3] I. Karla, J. Pierre, R.V. Skolozdra, J. Alloys Compd. 265, 42 (1998); https://doi.org/10.1016/S0925-8388(97)00419-2).
[4] R.V. Skolozdra, A. Guzik, A.M. Goryn, J. Pierre, Acta Phys. Polonica A 92, 343 (1997); https://doi.org/10.12693/APhysPolA.92.343.
[5] T. Harmening, H. Eckert, R. Pöttgen, Solid State Sci. 11(4), 900 (2009); https://doi.org/10.1016/j.solidstatesciences.2008.12.007.
[6] V.V. Romaka, L. Romaka, A. Horyn, P. Rogl, Yu. Stadnyk, N. Melnychenko, M. Orlovskyy, V. Krayovskyy, J. Solid State Chem. 239, 145 (2016); https://doi.org/10.1016/j.jssc.2016.04.029).
[7] V.V. Romaka, L. Romaka, A. Horyn, Yu. Stadnyk, J. Alloys Compd. 855, 157334 (2021); https://doi.org/10.1016/j.jallcom.2020.157334.
[8] L.I. Anatychuk, Thermoelements and thermoelectric devices (Naukova dumka, Kyiv 1979) [in Russian].

[9] T. Roisnel, J. Rodriguez-Carvajal, Mater. Sci. Forum, Proc. EPDIC7, 378-381, 118 (2001); https://doi.org/10.4028/www.scientific.net/MSF.378-381.118.
[10] V.P. Babak, V.V. Shchepetov, J. Friction and Wear. 39, 38 (2018); https://link.springer.com/article/10.3103/S1068366618010038.
[11] Yu. Stadnyk, L. Romaka, V.A. Romaka, A. Horyn, V. Krayovskii, P. Klyzub, M. Rokomanyuk, XXII Intern. Sem. Phys. Chem. Solids, June 17-19 (Lviv, Ukraine, 2020). P. 35.
[12] B.I. Shklovskii and A.L. Efros, Electronic Properties of Doped Semiconductors (Springer, NY, 1984).
[13] N.F. Mott and E.A. Davis, Electron Processes In Non-crystalline Materials (Clarendon Press, Oxford, 1979).

В.А. Ромака[1], Ю. Стадник[2], Л. Ромака[2], А. Горинь[2], В. Пашкевич[1], Г. Ничипорук[2], П. Гаранюк[1]

Дослідження термоелектричного матеріалу на основі твердого розчину $Lu_{1-x}Zr_xNiSb$. I. Експериментальні результати

[1]*Національний університет "Львівська політехніка", Львів, Україна, volodymyr.romaka@gmail.com;*
[2]*Львівський національний університет ім. І.Франка, Львів, Україна, lyubov.romaka@gmail.com*

Вивчено вплив легування фази пів-Гейслера *p*-LuNiSb (структурний тип MgAgAs) атомами Zr на структурні, кінетичні, енергетичні та магнітні характеристики напівпровідникового твердого розчину $Lu_{1-x}Zr_xNiSb$ у діапазонах: T = 80 - 400 K, x = 0 - 0,10. Експериментально встановлено, що при легуванні сполуки *p*-LuNiSb атомами Zr одночасно генеруються як структурні дефекти акцепторної природи, так і донорної, концентрація яких росте при збільшенні вмісту атомів Zr. Показано, що досліджений напівпровідниковий твердий розчин $Lu_{1-x}Zr_xNiSb$ є перспективним термоелектричним матеріалом.

Ключові слова: напівпровідник, електропровідність, коефіцієнт термо-ерс, рівень Фермі.